Using the current seasonal cycle to constrain snow albedo feedback in future climate change

Alex Hall and Xin Qu

Department of Atmospheric and Oceanic Sciences, University of California, Los Angeles, California, USA

Received 9 November 2005; revised 14 December 2005; accepted 28 December 2005; published 3 February 2006.

[1] Differences in simulations of climate feedbacks are sources of significant divergence in climate models' temperature response to anthropogenic forcing. Snow albedo feedback is particularly critical for climate change prediction in heavily-populated northern hemisphere land masses. Here we show its strength in current models exhibits a factor-of-three spread. These large intermodel variations in feedback strength in climate change are nearly perfectly correlated with comparably large intermodel variations in feedback strength in the context of the seasonal cycle. Moreover, the feedback strength in the real seasonal cycle can be measured and compared to simulated values. These mostly fall outside the range of the observed estimate, suggesting many models have an unrealistic snow albedo feedback in the seasonal cycle context. Because of the tight correlation between simulated feedback strength in the seasonal cycle and climate change, eliminating the model errors in the seasonal cycle will lead directly to a reduction in the spread of feedback strength in climate change. Though this comparison to observations may put the models in an unduly harsh light because of uncertainties in the observed estimate that are difficult to quantify, our results map out a clear strategy for targeted observation of the seasonal cycle to reduce divergence in simulations of climate sensitivity.
Citation: Hall, A., and X. Qu (2006), Using the current seasonal cycle to constrain snow albedo feedback in future climate change, *Geophys. Res. Lett.*, *33*, L03502, doi:10.1029/2005GL025127.

1. Introduction

[2] One reason convergence in simulations of climate feedbacks has eluded the climate modeling community [*Bony et al.*, 2006; *Stocker et al.*, 2001; *Bony et al.*, 2004] is the difficulty in evaluating the feedbacks against observations. Century-scale observations of variations in surface albedo, tropospheric water vapor, and clouds during the era of significant anthropogenic forcing would be necessary to evaluate feedbacks rigorously, and these are not available. We circumvent this by exploiting similarities between anthropogenic climate change and the present-day seasonal cycle. Both are examples of externally-forced climate variability, and it has been suggested that both are subject to the same climate feedbacks [*Tsushima et al.*, 2005]. Support for this idea has been found recently in correlations between simulated seasonal cycle amplitudes and sensitivity to external forcing in the current generation of climate models [*Knutti et al.*, 2006].

[3] In the case of snow albedo feedback (SAF), the seasonal cycle may be a particularly appropriate analog for climate change because interactions of northern hemisphere (NH) continental temperature, snow cover, and broadband surface albedo (α_s) in the context of the seasonal variation of insolation are strikingly similar to interactions of these variables in the context of anthropogenic forcing. In the current climate northern hemisphere (NH) snow cover retreats rapidly from a maximum in late winter to a minimum in late summer in direct response to increasing sunshine and associated warmer temperatures [*Robinson et al.*, 1993]. This in turn decreases α_s over NH continents, further increasing absorbed sunshine and enhancing surface warming. Similarly, in nearly all previous simulations of future climate [*Cess et al.*, 1991; *Randall et al.*, 1994; *Cubasch et al.*, 2001; *Manabe and Wetherald*, 1980; *Robock*, 1983; *Ingram et al.*, 1989], as well as those of the current Intergovernmental Panel on Climate Change Fourth Assessment Report (AR4), snow cover retreats almost simultaneously with anthropogenic warming over NH land masses, reducing α_s in these areas, and increasing the overall warming through enhanced absorption of solar radiation (Figure 1).

[4] SAF strength can be quantified, whether it occurs in the context of the current seasonal cycle or anthropogenic climate change. We set forth a method for doing this, and use the results to examine the simulated relationship between the strength of NH springtime SAF in climate change and seasonal cycle contexts in 17 models used in the AR4 assessment. (See Table 1 for a list of the models.) If the strength of SAF in the seasonal cycle in any particular model is correlated with its strength in climate change, then comparison of simulated SAF strength in the seasonal cycle to observations provides a meaningful constraint on simulated SAF strength in climate change. The seasonal cycle offers advantages in model-observation comparison because it recurs every year. The current satellite record is about two decades long, so that already enough seasonal cycle realizations have been sampled to provide statistically-stable estimates of SAF strength in the seasonal cycle context. We focus on the springtime component of NH SAF because both snow extent and insolation are large at this time. Hence SAF during springtime is particularly effective, contributing approximately half the total NH SAF to simulated global climate change [*Hall*, 2004].

2. SAF Components

[5] We quantify SAF strength by the variation in net incoming shortwave radiation (Q) with surface air temperature (T_s) due to changes in α_s [*Cess and Potter*, 1988]:

$$\left(\frac{\partial Q}{\partial T_s}\right)_{SAF} = -I_t \cdot \frac{\partial \alpha_p}{\partial \alpha_s} \cdot \frac{\Delta \alpha_s}{\Delta T_s} \tag{1}$$

where the subscript SAF is used to emphasize that the partial derivative refers only to changes in Q with T_s that occur due to

0094-8276/06/2005GL025127

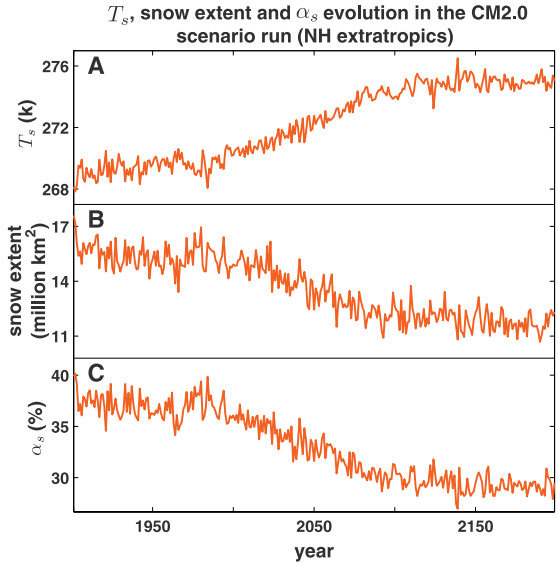

Figure 1. Time series of (a) springtime-mean (MAM) T_s, (b) snow extent, and (c) α_s averaged over NH continents poleward of 30°N simulated by the GFDL CM2.0 model. Time series of these quantities for the other 16 models of Table 1 are similar. Values of α_s were weighted by springtime-mean incoming insolation prior to averaging.

changes in α_s, rather than changes in cloud or other factors affecting solar radiation. The constant I_t is incoming solar radiation at the top of atmosphere (TOA), and α_p is planetary albedo. Equation (1) allows SAF to be decomposed as the product of two terms. The first ($\partial\alpha_p/\partial\alpha_s$) represents the atmosphere's attenuation effect on anomalies in α_s, determined by the time-mean distribution of solar absorbers, including cloud. The other ($\Delta\alpha_s/\Delta T_s$) is the change in α_s induced by a unit change in T_s, determined by surface processes.

[6] Recently a highly accurate technique was developed to calculate $\partial\alpha_p/\partial\alpha_s$ given standard model output (α_s, cloud cover and cloud optical thickness data, and TOA clear-sky and all-sky solar fluxes). We use it to calculate springtime $\partial\alpha_p/\partial\alpha_s$ values in NH land areas for AR4 transient climate change experiments (Figure 2a). The intermodel variation in this quantity is small, with most models agreeing to within 10% that a given α_s anomaly results in an α_p anomaly one-half as large. This agreement occurs because the main factor controlling $\partial\alpha_p/\partial\alpha_s$ is the cloudless component of the atmosphere, where the models' radiative transfer schemes converge in their handling of the atmosphere's interaction with upwelling solar photons [*Qu and Hall*, 2006]. Thus differences in cloud fields do not introduce significant differences in estimates of $\partial\alpha_p/\partial\alpha_s$. It is straightforward to calculate the second component of SAF ($\Delta\alpha_s/\Delta T_s$) in the climate change context based on springtime values of α_s and T_s averaged over NH land areas from the beginning and end of AR4 experiments (Figure 2b). While simulated estimates of $\partial\alpha_p/\partial\alpha_s$ generally agree, there is a three-fold divergence in $\Delta\alpha_s/\Delta T_s$, with no clear preference for a central value.

3. Seasonal Cycle and Climate Change Relationship

[7] Because the $\Delta\alpha_s/\Delta T_s$ component is most responsible for intermodel spread in SAF strength, we focus on this component in our assessment of SAF in seasonal cycle and climate change contexts. It is possible to calculate values of $\Delta\alpha_s/\Delta T_s$ in the seasonal cycle by taking climatological changes in NH continental α_s from one month to another and dividing them by climatological changes in T_s between the same two months. Consistent with our springtime focus, we did this for April and May based on the 20th century portion the AR4 experiments. This is a time of year when NH continental α_s decreases rapidly, while T_s increases quickly. Figure 3 shows a scatterplot of these values against the climate change values of $\Delta\alpha_s/\Delta T_s$ of Figure 2b. Intermodel variations in $\Delta\alpha_s/\Delta T_s$ in the seasonal cycle are highly correlated with $\Delta\alpha_s/\Delta T_s$ in climate change. Moreover, the best-fit regression line slope is nearly one, so values of $\Delta\alpha_s/\Delta T_s$ based on the present-day seasonal cycle are excellent predictors of the absolute magnitude of $\Delta\alpha_s/\Delta T_s$ in climate change. Apparently the snow pack's thermodynamic response time is fast enough that in every simulation the snow retreat and α_s reduction associated with springtime warming mimics closely the analogous process occurring in response to century-scale warming.

[8] To calculate an observed estimate of $\Delta\alpha_s/\Delta T_s$ in the seasonal cycle context, we took April and May α_s values from the satellite-based International Satellite Cloud Climatology Project (ISCCP). Nearly 20 years in length, this is the only observed time series long enough to provide a statistically stable estimate of climatological α_s. April and May climatological T_s is easily extracted from reanalysis data. We also calculated an estimate of the statistical error arising from the time series' limited length, giving a 95% confidence range. Three models are very close to the observed range, while eleven have a significantly weaker SAF than observed. Three models appear to have an unrealistically strong SAF, though no model's SAF is stronger than the observed range by more than 20%.

[9] Caution must be exercised in this comparison, because there may be error sources other than statistical uncertainty in the observed estimate of $\Delta\alpha_s/\Delta T_s$. Unfortunately these are nearly impossible to quantify, and must be

Table 1. Model Names Used for AR4 Climate Change Experiments[a]

Number	Name of Model
1	mri_cgcm2_3_2a
2	cnrm_cm3
3	giss_model_e_r
4	iap_fgoals1_0_g
5	cccma_cgcm3_1
6	csiro_mk3_0
7	ncar_pcm1
8	ukmo_hadcm3
9	mpi_echam5
10	ukmo_hadgem1
11	miroc3_2_medres
12	ncar_ccsm3_0
13	miub_echo_g
14	ipsl_cm4
15	gfdl_cm2_0
16	gfdl_cm2_1
17	inmcm3_0

[a]All data were taken from the '720 ppm stabilization experiment,' where historical 20th century forcing was imposed, followed by the SRES A1B emission scenario for the 21st century. At year 2100, anthropogenic forcings were fixed for the remainder of the experiments, which end at year 2200. Though this forcing scenario was imposed on 23 models for the AR4, only these 17 had a complete time series when this article was composed.

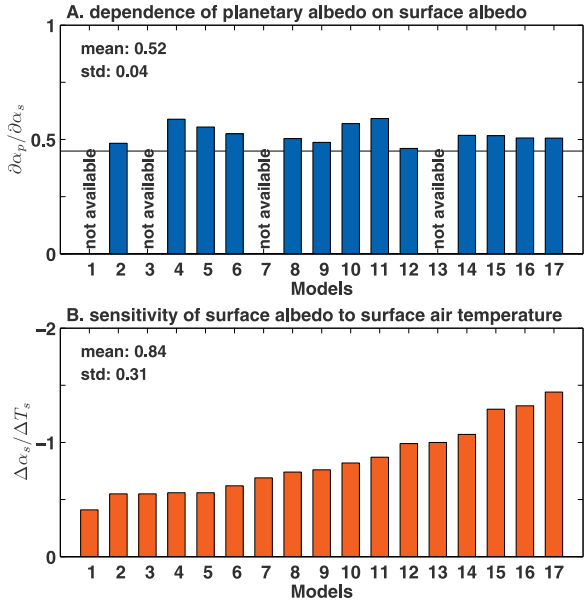

Figure 2. (a) Dependence of April α_p on α_s in NH land masses poleward of 30°N seen in AR4 experiments for the 20th century, showing how large a typical α_p anomaly is for a 1% α_s anomaly in areas likely to be affected by SAF. The data required for this calculation [*Qu and Hall*, 2006] were only available for 13 simulations. We performed the same calculation for other time periods (not shown), and found these values exhibit very little dependence on time period chosen. We also used this method to calculate $\partial\alpha_p/\partial\alpha_s$ from ISCCP data (1984–2000 period). This observed value (solid line) is in general agreement with simulated values. (b) The externally-forced change in April α_s (%) averaged over NH land masses poleward of 30°N in the AR4 experiments, divided by the change in April T_s in these experiments averaged over the same region. The change in α_s (or T_s) is defined as the difference between 22nd-century-mean α_s (T_s) and 20th-century-mean α_s(T_s). Values of α_s were weighted by April incoming insolation prior to averaging. Though these values of $\Delta\alpha_s/\Delta T_s$ are based on transient climate change experiments, they agree closely with the values of $\Delta\alpha_s/\Delta T_s$ that would result from equilibrium climate change experiments with the same models: In climate simulations the NH snow pack thermodynamically adjusts almost instantaneously to anthropogenic forcing [*Hall*, 2004]. The experiment names corresponding to numbers on the x-axis are given in Table 1.

evaluated qualitatively: Measurements of T_s are an unlikely source of systematic or random measurement error. T_s over the NH land masses is well-sampled in space and time and the measurements are accurate, so we expect the reanalysis to provide highly reliable estimates of climatological T_s. Additional evidence for this is that values of ΔT_s calculated from reanalysis agree nearly perfectly with those calculated from another standard T_s data set constructed by the University of East Anglia Climate Research Unit [*New et al.*, 2000]. Observations of α_s present a more likely error source. ISCCP α_s values are based on satellite measurements at a single visible channel, and a dependence of albedo on wavelength is assumed to convert these observations to a broadband value. This functional dependence is in turn derived from measurements of the Earth Radiation Budget Experiment, when shortwave fluxes were measured simultaneously with ISCCP at seven visible and near infrared channels for the 1984–1989 period [*Zhang et al.*, 2004]. This approach, though reasonable as reflectances measured at the ISCCP channel are highly correlated with reflectances at other wavelengths where solar energy is concentrated, may introduce errors. Because of these errors the actual uncertainty range in observed values of $\Delta\alpha_s/\Delta T_s$ may be somewhat larger than the range of Figure 3; however, it seems improbable that the range would broaden enough to include all models. For example, for models in the low end of the range of Figure 3 to be realistic, ISCCP's climatological seasonal reduction in α_s from April to May would have to be too large by a factor of two.

4. Concluding Remarks

[10] The difficulty in quantifying all errors in the estimate of climatological $\Delta\alpha_s/\Delta T_s$ points to a clear strategy for

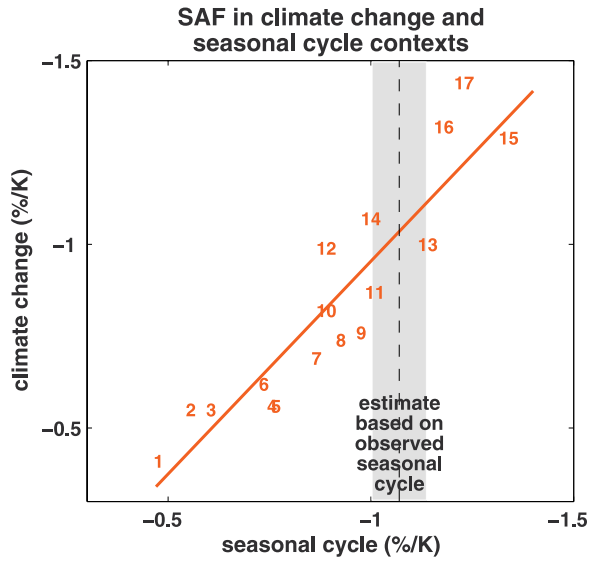

Figure 3. Scatterplot of simulated springtime $\Delta\alpha_s/\Delta T_s$ values in climate change (ordinate) vs. simulated springtime $\Delta\alpha_s/\Delta T_s$ values in the seasonal cycle (abscissa). The numbers of the 17 experiments (Table 1) are used as plotting symbols. The climate change $\Delta\alpha_s/\Delta T_s$ values are simply the data in Figure 2b. Seasonal cycle $\Delta\alpha_s/\Delta T_s$ values, based on 20th century climatological means, are calculated by dividing the difference between April and May α_s averaged over NH continents poleward of 30°N by the difference between April and May T_s averaged over the same area. Values of α_s were weighted by April incoming insolation prior to averaging. A least-squares fit regression line for the simulations is also shown. The two $\Delta\alpha_s/\Delta T_s$ parameters are highly correlated ($r^2 = 0.92$). The observed springtime $\Delta\alpha_s/\Delta T_s$ value based on ISCCP and the ERA40 reanalysis (see text) is plotted as a dashed vertical line. The grey bar gives an estimate of statistical error, calculated according to a standard formula for error in the estimate of the mean of a time series (in this case the observed time series of $\Delta\alpha_s/\Delta T_s$) given the time series' length and variance [*Neter et al.*, 1996]. If this statistical error only is taken into account, the probability the actual observed value lies outside the grey bar is 5%.

targeted observation of the climate system. A systematic campaign to establish the seasonal climatology of α_s with a high degree of precision and accuracy, either through improved utilization of existing measurements or new satellite instruments, will lead directly to identification of biases in simulations of SAF in the seasonal cycle. And the high correlation between simulated SAF parameters in seasonal cycle and climate change implies the models will converge in their simulations of SAF in climate change if these biases are addressed through a parallel program of model evaluation. Though detailed analysis of the cause of the wide divergence in simulated SAF strength is beyond the scope of this paper, preliminary results indicate SAF strength is correlated with prescribed α_s values for deep snow. When these values are small, the albedo contrast between snow-covered and snow-free areas decreases, weakening SAF. Therefore biases in SAF strength may be linked to easily identifiable errors in models. This gives hope that the biases may be easily corrected, reducing the divergence in simulations of future climate in large portions of heavily-populated northern hemisphere land masses, where SAF may account for nearly half the simulated anthropogenic warming [*Hall*, 2004].

[11] Exploiting similarities between the seasonal cycle and anthropogenic climate change is a promising strategy for constraining other radiative feedbacks affecting the extratropics, where seasonality is most pronounced. For example, sea ice albedo feedback is a significant source of divergence in simulations of climate sensitivity to anthropogenic forcing in high latitudes [*Holland and Bitz*, 2003], and is typically larger than snow albedo feedback in climate change simulations. Like NH snow, sea ice in both hemispheres undergoes a large variation in response to the seasonal cycle of extratropical temperatures. If sea ice albedo feedback could be also constrained with the current seasonal cycle, this would substantially reduce divergence in simulations of extratropical climate change.

[12] **Acknowledgments.** Alex Hall and Xin Qu are supported by NSF ATM-0135136. Opinions, findings, conclusions, or recommendations expressed here are those of the authors and do not necessarily reflect NSF views. We thank the modeling groups for providing data, PCMDI for collecting and archiving this data, JSC/CLIVAR WGCM and their CMIP and Climate Simulation Panel for organizing the model analysis, and the IPCC WG1 TSU for technical support. The IPCC data archive at Lawrence Livermore National Laboratory is supported by the US Department of Energy.

References

Bony, S., et al. (2004), On dynamic and thermodynamic components of cloud changes, *Clim. Dyn.*, *22*, 71–86.

Bony, S., et al. (2006), How well do we understand climate change feedback processes?, *J. Clim.*, in press.

Cess, R. D., and G. L. Potter (1988), A methodology for understanding and intercomparing atmospheric climate feedback processes in general circulation models, *J. Geophys. Res.*, *93*(D7), 8305–8314.

Cess, R. D., et al. (1991), Interpretation of snow-climate feedback as produced by 17 general circulation models, *Science*, *253*, 888–892.

Cubasch, U., et al. (2001), Projections of future climate change, in *Climate Change 2001: The Scientific Basis*, edited by J. W. Kim and J. Stone, pp. 525–582, Cambridge Univ. Press, New York.

Hall, A. (2004), The role of surface albedo feedback in climate, *J. Clim.*, *17*, 1550–1568.

Holland, M. M., and C. M. Bitz (2003), Polar amplification of climate change in coupled models, *Clim. Dyn.*, *21*, 221–232.

Ingram, W. J., C. A. Wilson, and J. F. B. Mitchell (1989), Modeling climate change: An assessment of sea ice and surface albedo feedbacks, *J. Geophys. Res.*, *94*(D6), 8609–8622.

Knutti, R., G. Meehl, M. Allen, and D. Stainforth (2006), Constraining climate sensitivity from the seasonal cycle in surface temperature, *J. Clim.*, in press.

Manabe, S., and R. T. Wetherald (1980), On the distribution of climate change resulting from an increase in CO_2 content of the atmosphere, *J. Clim.*, *37*, 99–118.

Neter, J., et al. (1996), Inferences in regression analysis, in *Applied Linear Statistical Models*, 4th ed., pp. 44–94, McGraw-Hill, New York.

New, M., M. Hulme, and P. Jones (2000), Representing twentieth-century space-time climate variability. Part II: Development of 1901–96 monthly grids of terrestrial surface climate, *J. Clim.*, *13*, 2217–2238.

Qu, X., and A. Hall (2006), Assessing snow albedo feedback in simulated climate change, *J. Clim.*, in press.

Randall, D. A., et al. (1994), Analysis of snow feedbacks in 14 general circulation models, *J. Geophys. Res.*, *99*(D10), 20,757–20,772.

Robinson, D. A., K. F. Dewey, and R. R. Heim Jr. (1993), Global snow cover monitoring: An update, *Bull. Am. Meteorol. Soc.*, *74*(9), 1689–1696.

Robock, A. (1983), Ice and snow feedbacks and the latitudinal and seasonal distribution of climate sensitivity, *J. Atmos. Sci.*, *40*, 986–997.

Stocker, T. F., et al. (2001), Physical climate processes and feedbacks, in *Climate Change 2001: The Scientific Basis*, edited by S. Manabe and P. Mason, pp. 417–470, Cambridge Univ. Press, New York.

Tsushima, Y., A. Abe-Ouchi, and S. Manabe (2005), Radiative damping of annual variation in global mean temperature: Comparison between the observed and simulated feedback, *Clim. Dyn.*, *24*, 591–597.

Zhang, Y.-C., W. B. Rossow, A. A. Lacis, V. Oinas, and M. M. Mishchenko (2004), Calculation of radiative fluxes from the surface to top of atmosphere based on ISCCP and other global datasets: Refinements of the radiative transfer model and the input data, *J. Geophys. Res.*, *109*, D19105, doi:10.1029/2003JD004457.

A. Hall and X. Qu, Department of Atmospheric and Oceanic Sciences, University of California, Los Angeles, PO BOX 951565, CA 90095-1565, USA. (alexhall@atmos.ucla.edu)